

# Aging Analysis in Large-scale Wireless Sensor Networks<sup>\*</sup>

Jae-Joon Lee<sup>\*</sup> Bhaskar Krishnamachari C.-C. Jay Kuo

*Department of Electrical Engineering, University of Southern California*

---

## Abstract

Most research on the lifetime of wireless sensor networks has focused primarily on the energy depletion of the very first node. In this study, we analyze the entire aging process of the sensor network in a periodic data gathering application. In sparse node deployments, it is observed that the existence of multiple alternate paths to a sink leads to a power law relation between connectivity to a sink and hop levels, where the probability of connection to a sink decreases in proportion to the hop level with an exponent, when device failures occur over time. Then, we provide distance-level analysis for the dense deployment case by taking into account the re-construction of a data gathering tree and workload shift caused by the energy depletion of nodes with larger workload. Extensive simulation results obtained with a realistic wireless link model are compared to our analytical results. Finally, we show through an analysis of the aging of first-hop nodes that increasing node density with a fixed radio range does not affect the network disconnection time.

*Key words:* Wireless sensor networks, Aging process, Reliability, Data gathering tree, Connectivity, Residual energy, Network lifetime

---

## 1 Introduction

A wireless sensor network typically consists of a large number of low-cost sensor devices with limited battery energy deployed in an unattended manner. Many applications require sensor nodes to operate in the context of limited

---

\* A portion of Section 3.1 and 3.2 in this paper was presented at IEEE VTC, Los Angeles, CA, September 2004.

<sup>\*</sup> Corresponding author.

Email addresses: jaejlee@usc.edu (Jae-Joon Lee), bkrishna@usc.edu (Bhaskar Krishnamachari), cckuo@sipi.usc.edu (C.-C. Jay Kuo).

resources, node failure and an unpredictable dynamic environment in a distributed and self-organized way [1, 2]. Under the above constraints, a sensor network should provide a certain degree of network performance required by applications for a target period of time. The aging problem is important in the fields of biology [3–5] and system reliability [6] and has been extensively studied therein. Studies in biology and system reliability have attempted to understand the causes of the aging process and predict the lifetime of organisms or systems by characterizing their aging process. According to the Gompertz law [7], the living adult organism’s mortality rate increases exponentially with age.

A similar aging phenomenon occurs in wireless sensor networks. Since the aging process of a network is caused by the aging of its constituent sensor nodes, we need to examine the aging process of each individual node, including the energy consumption rate and the device reliability rate. The energy consumption rate is however not a trivial problem since a sensor network has to be regarded as a whole system (or an organism) that allows dynamic interaction among sensors with respect to the evolving nature of the environment and the survival state of neighboring nodes. To analyze the aging process of a wireless sensor network, we would like to understand how nodes approach the end of their life and how the network performance degrades over time. Generally speaking, we have to examine this problem from a microscopic view of energy consumption or reliability in a sensor device as well as a macroscopic view of the network environment and condition in order to understand the overall aging process of a network. Applications, operations, the initial deployment, and the operating environment all affect the aging process. With a good understanding of the aging process and an accurate prediction, we can provide proper network maintenance planning and operations effectively, which include energy-efficient operations such as load balancing and power saving to delay the aging process as well as proper planning in redeployment and/or recharging time to extend the network’s life. Predicting when and where nodes are approaching to death can enable timely network maintenance without interrupting network operations.

In this work, we extensively examine aging beyond initial node death due to energy depletion and device failure in diverse network operations and deployment conditions. It reveals that diverse aging phenomena depend on network conditions including multi-hop communication with sparse and dense node deployments.

- In a multi-hop data gathering tree for a sparse node deployment, we present hop level analysis of workload. We discuss the effect of energy depletion with or without data aggregation and the effect of device failure on the connection at each hop level to a sink in the tree. A power law is observed in the relation between connectivity and the hop level in the face of node

death caused by device failure and energy depletion with data aggregation as node death increases, which is due to the existence of multiple alternate paths to the sink. Thus, the probability of connection to the sink decreases in proportion to the hop level with an exponent. From these observations, we characterize connectivity to a sink in each hop level over time after the initial node death.

- In the dense node deployment case with a multi-hop data gathering tree, the finer-grained distance level workload distribution among survivor nodes over time is analyzed by incorporating the effect of dynamic tree reconstruction caused by the death of other nodes. With mathematical analysis, we can predict the energy consumption distribution and the residual energy distribution over time and space in a large-scale wireless sensor network with low complexity. Besides theoretical analysis, we provide simulation results using a realistic wireless link model. In addition, our first-hop node aging analysis in a dense deployment provides the expression of the node density effect on the network disconnection time and the prediction of disconnection time caused by energy depletion.

The rest of this paper is organized as follows. Previous work on energy consumption and lifetime analysis, and connectivity is reviewed in Section 2. Section 3 provides hop-level analysis for sparse node deployment. Then, finer-grained distance-level analysis for dense node deployment is discussed in Section 4. Finally, conclusion and future research directions are presented in Section 5.

## 2 Related Work

The energy consumption model and the network lifetime analysis until the first node death have been studied in [8–11]. Heinzelman *et al.* [8] present a general energy consumption model for communication components in a sensor device and analyzed the cluster-based data gathering scheme. Bhardwaj and Chandrakasan [9] discuss the upper bound of the network lifetime by considering the network topology and the data aggregation scheme. They used the optimization model to compute the maximum lifetime of a sensor network. Lotfinezhad and Liang [10] analyze the energy consumption of data forwarding with a distance level when all nodes are alive, and showed that high energy consumption is required in the outer border of each hop level when a random parent selection scheme is used. Several operational modes of a sensor node, including sleep and active modes, are modeled in [11] as a Markov chain and the energy dissipation level is computed with stationary probabilities of operational modes. The data communication rate of a node is derived using a network model, where parameters is obtained through iterations of a closed loop of a node model, a wireless link interference model and a network model.

Chen and Zhao [12] present the average network lifetime that incorporates the average unused energy in the network and the expected energy consumption. The lifetime expression is a general form that is independent of underlying networks. Using the expression, they propose a lifetime maximization MAC protocol. Zhang and Hou [13] study the node density and the lifetime upper bound that maintains a certain portion of network area to be covered. Olariu and Stojmenovic [14] present the discussion about the effect of the power attenuation factor and the way to balance the energy expenditure across hop levels by adjusting corona width in each hop level. Chen *et al.* [15] examine the effect of increasing number of nodes on network lifetime and present the optimal placement and number of nodes that maximize the network lifetime divided by total number of nodes deployed. While there are several papers that discuss the problem of non-uniform energy consumption across the network, our focus is to examine the aging process dealing with the effect of node deaths on the network and survivor nodes over time after the initial node death.

Many studies on connectivity have focused on identifying a proper radio range to achieve the connectivity between any two nodes in an uniformly distributed sensor environment at the deployment time [16, 17]. Gupta and Kumar [16] present the condition for transmission power that ensures a network is connected with probability one. Bettstetter [17] derives the expression for the probability of the minimum node degree and a k-connected network of a certain radio range and node density using the Poisson point formulation. There is some research on the network performance degradation process caused by the node death [18, 19]. Shakkottai *et al.* [18] use a node failure rate to derive a bound on the probability for all nodes to be connected and the network to be covered in a grid deployment. Their main result shows that the network is connected and covered if the transmission radius multiplied by the square root of the node survival probability is of order  $\sqrt{\log(n)/n}$ . Kunniyur and Venkatesh [19] analyze network devolution caused by node death and examined the transitional behavior of connectivity between live nodes. The battery lifetime of nodes is assumed to be an independent random variable, which is basically identical to the device reliability model. Our work focuses on the connectivity aging process over time in the face of nodes death either due to energy depletion or device failure.

### 3 Hop-Level Aging Analysis for Sparse Node Deployment

The aging process in a multi-hop data gathering tree with a sink is presented. First, hop-level analysis for sparse node deployment is examined. It is assumed that nodes are deployed uniformly at random. A data gathering tree is shown in Fig. 1. It is formed such that all deployed sensor nodes are connected to

a sink, and can be constructed as follows. First, we find the set of first hop nodes that can directly connect to the sink within its radio range. Then, other nodes select the parent nodes that are within their radio range and have a shorter hop level from the sink to establish the forwarding path to the sink [20]. In wireless sensor networks, major energy consumption activities include communications, data processing and sensing. The communication plays a dominant role in the battery energy consumption [21] as compared to other activities, and the data gathering communication towards a sink accounts for the major portion of communication in most wireless sensor networks. Thus, the average number of children and descendants provides a good estimation of workload in each hop level. We assume that every node periodically generates one data unit and sends it to the sink in each data sampling *round*, which is adopted as the discrete time unit  $t$ .

### 3.1 Workload at Each Hop Level

As shown in Fig. 1, the area of the  $h$ -hop level from the sink can be computed via

$$h^2\pi r^2 - (h-1)^2\pi r^2 = (2h-1)\pi r^2, \quad h = 1, 2, 3, \dots$$

By assuming that the average number of nodes at each hop level is proportional to its area, the average child number of a node in hop level  $h$  can be computed as  $n_h^c = \frac{2h+1}{2h-1}$ . Then, we can obtain the average number of descendants ( $n_h^d$ ) of a node in hop level  $h$  as

$$n_h^d = \sum_{i=h}^{L-1} \left( \prod_{j=h}^i n_j^c \right) = \frac{L^2 - h^2}{2h-1}$$

where  $L$  is the maximum hop level from the sink.

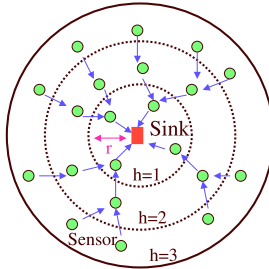


Fig. 1. The illustration of a data gathering tree, where  $h$  represents the hop level from the sink and  $r$  indicates the radio range of a sensor device.

If no data aggregation takes place during data forwarding, then the number of descendants of a node would determine the communication workload. When perfect data aggregation is performed, which aggregates multiple data received from children into one data unit (*e.g.*, MIN, MAX, SUM) [22], the number

of packets handled by a node is determined by the number of children. Thus, even in the case of perfect data aggregation the workload (amount of data communication) in the first hop nodes is at least twice as much as that in the other hop level nodes. Non-uniform density deployment and a sleep scheduling scheme for balancing energy consumption among the hop levels may use this approximate analysis of average workload. We further analyze the dynamic energy consumption in finer-grained distance level in Section 4.

### 3.2 Device Reliability

A low-cost sensor device is vulnerable to failure due to external or internal problems. Sensor devices can be deployed in diverse environments including hostile areas. The external environment such as temperature, pressure, etc. can produce device malfunctions. The device can also experience software failure, which prevents some required operation.

In this work, we model the reliability of a sensor node using a classical distribution known as the Weibull distribution [6]. Since the Weibull distribution can provide diverse failure patterns over time with its parameters, it is extensively used in reliability modelling. The probability density function of the Weibull distribution has the following form:

$$f(t) = \frac{\beta}{\eta} \left(\frac{t}{\eta}\right)^{\beta-1} e^{-(\frac{t}{\eta})^\beta},$$

where  $\beta$  and  $\eta$  are the shape and the scale parameters, respectively. This function indicates the likelihood of failure at time  $t$ . When  $\beta = 1$ , the  $f(t)$  is equal to the exponential distribution. The reliability function of the Weibull distribution is given by

$$R(t) = e^{-(\frac{t}{\eta})^\beta},$$

which is the complement of the cumulative distribution function of  $F(t)$  of the Weibull density function. The reliability function is the probability that a device is functioning at time  $t$ . The failure rate function is  $z(t) = f(t)/R(t)$ , which is the probability that an item fails when the item is functioning at time  $t$ . When the shape parameter  $\beta = 1$ , the failure rate is constant, and when  $\beta > 1$ , the failure rate increases over time. The sensor node survival function, denoted by  $S_i(t)$ , characterizes the node aging process in a data gathering tree. It is defined as the probability that node  $i$  is functioning at the data sampling round  $t$ . This function is primarily dependent on the energy consumption rate and the device reliability of a node. Initially, when  $t = 0$ ,  $S_i(0) = 1$ . For  $t > 0$ ,  $S_i(t)$  is  $R_i(t)$  if there exists residual energy and  $R_i(t)$  is the reliability function and otherwise,  $S_i(t) = 0$ .

Let  $C_i^h(t)$  be the event where node  $i$  in hop level  $h$  is connected to the sink

at time  $t$ . We use  $p_i^{h-1}$  to refer to any candidate ascendent nodes available in hop level  $h - 1$  of node  $i$  in a dynamic data gathering tree, which is within a radio range of node  $i$ . Then, we have

$$Pr(C_i^h(t)) = \begin{cases} S_i^h(t), & h = 1, \\ Pr(\bigcup C_{p_i^{h-1}}^{h-1}(t))S_i^h(t), & h \geq 2. \end{cases} \quad (1)$$

As given above, the probability that a node is connected to the sink is equal to the probability that any of the candidate parents is connected and the node is alive. The lower bound of Eq. (1) is the case where there is only one available parent for all nodes in the forwarding path, and it can be written as

$$Pr(C_i^h(t)) \geq (\prod_{k=1}^{h-1} S_{p_i^k}^k(t))S_i^h(t), \quad h > 1 \quad (2)$$

A more general expression for the connectivity probability at hop level  $h$  over time,  $Pr(C^h(t))$ , which provides average value for each hop level, can be expressed as

$$Pr(C^h(t)) = \begin{cases} S^h(t), & h = 1, \\ (1 - (1 - Pr(C^{h-1}(t)))^{n_p})S^h(t), & h \geq 2, \end{cases} \quad (3)$$

where  $n_p$  is the expected number of available candidate parents in the upper hop level. When  $n_p = 1$ ,  $Pr(C_h(t))$  becomes the lower bound as Eq. (2).

### 3.3 Analysis Validation

Fig. 2(a) shows the connection probability in a data gathering tree in each hop level according to Eq. (3) where  $n_p$  is set to 2. In this figure, all nodes have the uniform survival function that follows the Weibull reliability function with  $\eta = 160$  and  $\beta = 3$  regardless of hop levels. The simulation results given in Fig. 2(b) and the analytical results given in Fig. 2(a) are consistent in their overall shape and the decreasing pattern of the differences between adjacent hop levels. It is observed that the connection probability becomes similar as hop level increases, which is characterized in the following subsection. The simulation results are obtained as the average of 50 different random node deployments where each simulation runs for 200 rounds with 1600 nodes which are distributed uniformly at random. The radio range is set to provide around 9 neighboring nodes within the range on the average and the average furthest

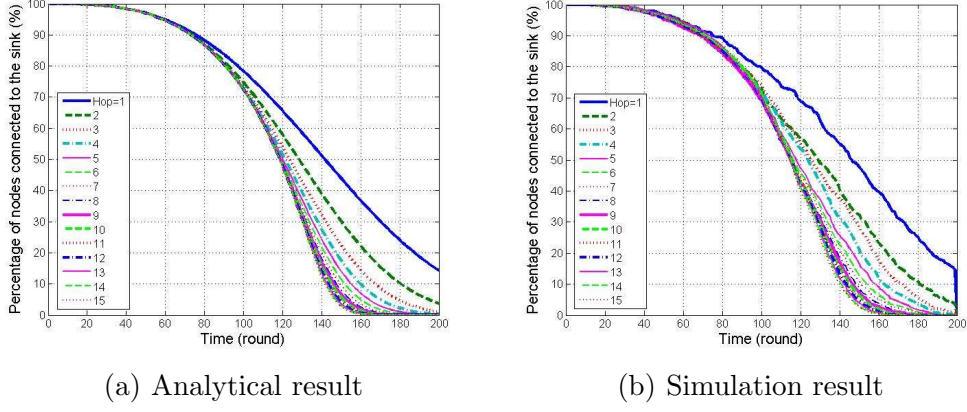


Fig. 2. The percentages of node connection in each hop level to the sink in the case of device reliability effect: (a) analytical and (b) simulation results.

hop level from the sink is around 16 in the complete circle network where the sink is located at the center.

In order to examine the effect of energy depletion of nodes on connectivity, we also performed two different energy consumption cases - with perfect data aggregation and without data aggregation with the same network simulation setup (50 different random deployments of 1600 nodes) as device random failure case. Energy consumption of a node  $i$  during the sampling round at  $t$  can be calculated using the number of communicated data units and the constant energy operation assumption as

$$\begin{aligned} E_i(t) &= E_{rx} \cdot n_i(t) + E_{tx} \cdot (1 + n_i(t)) + E_{other} \\ &= 2c_1 \cdot E_{elec} \cdot n_i(t) + c_2 \cdot E_{amp} \cdot (1 + n_i(t)) \cdot r^\kappa + E_{other}, \end{aligned} \quad (4)$$

where  $E_{rx}$  and  $E_{tx}$  denote the amount of energy consumption per data unit for receiving and transmitting, respectively,  $E_{other}$  is the energy consumption for non-communication operations such as sensing.  $n_i(t)$  represents the amount of data packet received from the children of the node  $i$ . As explained in Section 3.1,  $n_i(t)$  would be proportional to the number of children in case of perfect data aggregation or to the number of descendants in the case without data aggregation. Please note that a data unit generated by itself is added to the number of data packets received in data transmission. Furthermore, it was described in [8] that data transmission and reception can be expressed by an electronic operation and an amplifying operation. They are accounted for by  $E_{elec}$  and  $E_{amp}$ , respectively. Finally,  $c_1$  and  $c_2$  are constant factors and  $\kappa$  is the path loss exponent in Eq. (4). Eq. (4) can be re-written to the following simplified expression:

$$E(d, t) = E_1 \cdot n(d, t) + E_2 \cdot (1 + n(d, t)) \cdot r^\kappa + E_{other}, \quad (5)$$

where  $E_1$  is the energy required for distance-independent operations, and  $E_2$  is the energy for the amplifying portion. The parameters of the network are given below.  $\kappa = 2$ ,  $E_1 = 1$ ,  $E_2 = 0.001$  and  $E_{other} = 1$ . Please note that  $E_1$  and  $E_2$  are chosen based on the work in [8], where  $E_{elec} = 50nJ/bit$  and  $E_{amp} = 100pJ/bit/m^2$ . Simulation results for energy depletion cases are presented in Appendix A.

### 3.4 Connectivity Aging Function

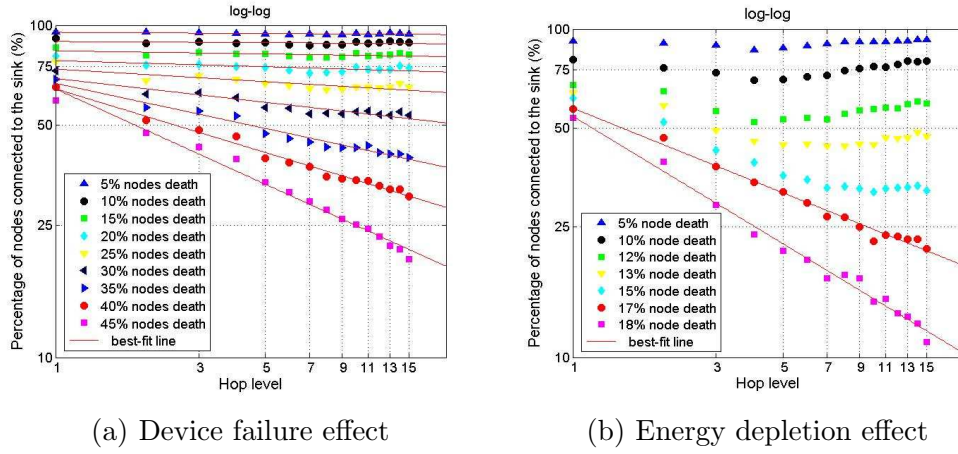


Fig. 3. The log-log plot of the percentages of node connection to the sink in each hop level over time as node death occurs due to (a) the device failure effect (80% of the node becomes disconnected with over 45% of the node deaths), and (b) the energy depletion effect, where perfect data aggregation is performed (80% of the node becomes disconnected with over 18% of the node deaths). The curves are obtained by the least-squares approximation.

A power-law relationship is observed between the connectivity and the hop level when node death occurs due to device failure from the log-log plots in Fig. 3(a). The figure shows that the probability of connection to a sink decreases in proportion to the hop level with an exponent as node death occurs. The least-squares approximation using linear regression provides straight lines that fit simulation data in these two plots. The power law between connectivity and the hop level can be well conjectured from this observation. Fig. 3(a) shows up to 45% node death case since around 45% of node death results in the disconnection of almost 80% of nodes. This power-law relation can be explained as follows. In the device uniform random failure case, the same percentage of node death occurs in all hop levels, which are included in disconnected nodes. In addition, as hop levels increase, the percentage of connected nodes decreases and its decreasing rate in the longer hop level saturates faster than the exponentially decaying curve, which is the lower bound of the connectivity function as shown in Eq. (2), since multiple candidate parents exist to re-construct the data forwarding path to the sink.

In case of the energy depletion effect with perfect data aggregation in Fig. 3(b), the longer hop level nodes show higher connectivity to the sink since most node deaths occur in the closer hop levels to the sink. Since over 80% of nodes become disconnected after 18% of node death, the connectivity up to 18% of node death is shown in this figure. The reason for the higher connectivity in the longer hop level up to 15% of node death in the figure is that most energy depletion occurs in the hop levels closer to the sink, which decreases the connectivity in those hop levels, while most nodes in the longer hop level are alive and find alternate routes to the sink which result in higher connectivity. However, as more node deaths occur (over 17% of node death), a similar power-law relationship is observed. If no data aggregation is performed, most of initial node deaths occur in the first-hop nodes and this results in drastic connectivity loss of all hop level nodes which have maintained higher connectivity except the first-hop level nodes. On the other hand, with perfect data aggregation, energy depleted nodes exist in all hop levels with much less difference than in the case without data aggregation.

**Definition 1** *The **connectivity aging function**, denoted by  $Pr(C^h(t))$ , is defined as the probability that a node in hop level  $h$  is connected to the sink at time  $t$ .*

When nodes die due to the uniform random device failure, the connectivity aging function  $Pr(C^h(t))$  at time  $t$  decreases as hop level  $h$  increases at each time instance. Their relationship can be expressed as

$$Pr(C^h(t)) \propto h^{-H(t)}, \quad H(t) \geq 0, \quad (6)$$

where  $H(t)$  is called the hop connectivity exponent and  $-H(t)$  indicates the slope of the log-scale plot for the percentage of nodes that are connected to the sink with respect to the hop level at each time. As to the device reliability effect,  $H(t)$  also depends on the device reliability function, which can be characterized by the Weibull distribution according to the device's characteristics and environmental conditions as explained in Section 3.2. Sparse node deployments, *e.g.*, 10 or less neighboring nodes, would result in the above relationship. Generally speaking, more densely deployed networks can maintain higher connectivity to the sink in the longer hop level nodes against node death.

The multi-hop tree structure for data gathering to a sink requires a proper function of first hop nodes to maintain the connectivity from the other nodes. In the sparse node deployment case, frequent redeployment will be needed to preserve the longer-hop's connectivity to a sink since the small fraction of node death can cause the connectivity loss in the longer hop levels. This can be characterized and predicted using the presented power-law relation in the case of random device failure. On the other hand, dense node deployment can

maintain the initial network connectivity from longer hop level until most of the first-hop nodes die, which is examined in the next section.

#### 4 Distance-Level Dynamic Aging Analysis for Dense Node Deployment

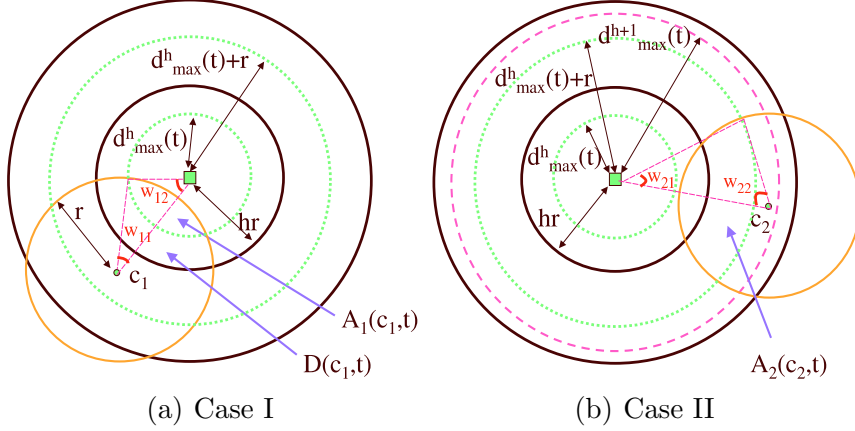


Fig. 4. Selection of a new parent after energy depletion of the current parent (a) Case I: Select a new parent in the live upper hop level (b) Case II: Select a new parent in the previously same hop level

In comparison to the sparse node deployment case, the dense node deployment case shows the larger difference of energy consumption amount among nodes of the same hop level, which leads to slower and gradual energy depletion of nodes over time. Thus, in this section, we examine finer-grained distance level node aging in a data gathering tree by analyzing the dynamic energy consumption change beyond the initial node death with tree re-construction. Then we examine the effect of the workload distribution and the node density on the aging process in the first-hop nodes, which determine the connection of the whole network.

##### 4.1 Finer-grained Dynamic Aging Analysis

In the following analysis, we consider the distance-level dynamic change of the number of descendants caused by the re-construction of the data gathering tree due to the death of other nodes. This process is illustrated in Fig. 4, where the center is the sink location and  $r$  is the radio range, and other notations are summarized in Table 1.

It was observed in [10] that energy consumption is the highest at the border of each hop level when the random parent selection scheme is used for minimum-

Table 1  
Summary of notation for a multi-hop communication tree.

$d$	distance from the sink
$c$	distance from the sink at which the children of a node at $d$ is located
$n(d, t)$	number of descendants of a node at distance $d$ and sampling round $t$
$n_0(d, t)$	$n(d, t)$ with the children that join before initial node death
$n_1(d, t)$	$n(d, t)$ with the children that newly join from the next hop area
$n_2(d, t)$	$n(d, t)$ with the children that newly join from the previous same hop area
$A(c)$	upper hop area within the radio range of a node at $c$
$A_1(c, t)$	live upper hop area within the radio range
$A_2(c, t)$	live same hop area within the radio range
$D(c, t)$	energy depleted upper hop area within the radio range
$d_{\max}^h(t)$	maximum distance of live nodes in hop level $h$
$\Delta d$	distance unit
$C(d, c)$	area between $c - \Delta d$ and $c$ and within the radio range of a node at $d$

hop data gathering tree construction as discussed in Section 3. The workload difference among nodes of the same hop level leads to gradual energy depletion of nodes from the border of each hop level and the workload change over time. The maximum distance of live nodes at hop level  $h$  over time is denoted by  $d_{\max}^h(t)$ .

Fig. 4 shows two cases of data gathering tree re-construction caused by energy depletion of some nodes.

- Case I:

Consider a node in hop level  $h + 1$  at distance  $c_1$  from the sink that has a parent node in area  $D(c_1, t)$ , where all nodes deplete their energy. Thus, it has to select a new parent in area  $A_1(c_1, t)$ , where nodes still have energy. This re-construction process increases the energy consumption of live nodes in that area.

- Case II:

Consider another node at distance  $c_2$ , which is located between  $d_{\max}^h(t) + r$  and  $d_{\max}^{h+1}(t)$ . If all nodes in the upper hop region within its radio range deplete their energy, nodes that lose their parent should select a new parent in area  $A_2(c_2, t)$ , which was in the same hop level previously, to forward the data towards the sink. This process splits one hop level into two.

To compute the expected number of children that are connected to a node, we can follow the analysis in [10], which provides the average number of de-

scendants of a node at distance  $d$  from the sink before any node death. This number is denoted by  $n_0(d)$ . Let  $Pr(A(c))$  be the probability that a node at distance  $c$  from the sink selects one node in the upper hop area  $A(c)$  to the sink within its radio range following [10], which is presented in Appendix B.

We use  $n_1(d, t)$  to denote the newly added number of descendants of a node at  $d$  for the first case in Fig. 4, where nodes at  $c_1$  select a new parent in area  $A_1$ .  $Pr(D(c, t))$  is the probability that node  $c_1$  selected a parent which was located in area  $D(c, t)$  in the upper hop area, which is  $\frac{D(c_1, t)}{D(c_1, t) + A_1(c_1, t)}$ . Then, we have

$$n_1(d, t) = \sum_{c=hr+\Delta d}^{d+r} \{C(d, c)\lambda(1 + n(c, t))Pr(D(c, t))Pr(A_1(c, t))\}, \quad (7)$$

where  $(h - 1)r < d < d_{\max}^h(t)$ ,  $h$  is the hop level of the node at  $d$ ,  $\lambda$  is the node density,  $C(d, c)$  is the area between  $c - \Delta d$  and  $c$  from the sink and within the radio range of the node at  $d$ , and  $n(c, t)$  is the number of descendants of a node at  $c$ , which can be calculated recursively. Basically, if the children of a node at  $d$  exist in the area from  $hr$  to  $d + r$  and within its radio range, we add the number of their descendants.

If there is no node available in the upper hop level, a child node will select a parent among nodes in the same hop level, which is the second case given in Fig. 4. As shown in the figure, node  $c_2$  will select a new parent in area  $A_2(c, t)$ . Let  $n_2(d, t)$  be the newly added number of descendants from the same hop level before initial node death. Then, we can derive the following

$$n_2(d, t) = \sum_{c=d_{\max}^{h-1}(t)+r+\Delta d}^{d_{\max}^h(t)} \{C(d, c)\lambda(1 + n(c, t))Pr(A_2(c, t))\}, \quad (8)$$

where  $(h - 1)r < d < d_{\max}^{h-1}(t) + r$ . In words, if the children of a node at  $d$  exist in the area from  $d_{\max}^{h-1}(t) + r$  to  $d_{\max}^h(t)$  and within its radio range, we add the number of their descendants.

Areas  $C(d, c)$ ,  $D(c, t)$ ,  $A(c)$ ,  $A_1(c, t)$  and  $A_2(c, t)$  can be computed based on geometry. These calculations are presented in Appendix B. Then, the average number of descendants of a node at  $d$ , denoted by  $n(d, t)$ , is the sum of three types of descendants obtained above, i.e.  $n(d, t) = n_0(d, t) + n_1(d, t) + n_2(d, t)$ . Energy consumption  $E(d, t)$  during the sampling round at  $t$  can be calculated as Eq. (5) and the value  $E(d, t)$  of nodes in a live region is recomputed whenever energy depletion of some node occurs. The energy depletion time of nodes is determined by the cumulative effect of the energy consumption dynamics among nodes over time.

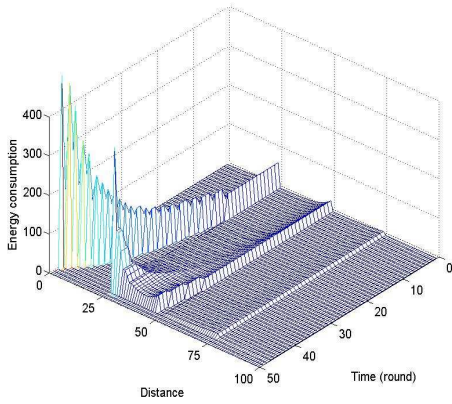


Fig. 5. The energy consumption distribution as a function of time and the distance from the sink.

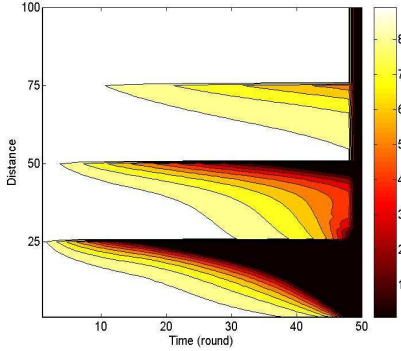


Fig. 6. The residual energy distribution (in terms of percentages) as a function of time and the distance from the sink.

#### 4.2 Understanding Network Aging via Case Study

We evaluate the performance of a wireless sensor network based on our analysis conducted above by considering an example. The parameters of the network are given below. The radio range  $r$  is 25m, the network radius is 100m from the sink, a total of 500 nodes are deployed and the other parameters follow the values used in Section 3.3.

The energy consumption distribution as a function of time and the distance from the sink is shown in Fig. 5. As shown in the figure, the energy consumption rate is significantly larger for nodes in the first and the second hop levels of the sink. As time increases, nodes in the initial second hop area are split into two groups. One is directly connected to the first hop nodes while the other is not due to the energy depletion of nodes in the border of the first hop area. It is also worthwhile to point out the high energy consumption for nodes in the second hop close to the first hop border, which is caused by the rapid increase of newly joined descendants,  $n_2(d, t)$ , from the same hop area previously.

The residual energy distribution as a function of time and the distance from the sink is shown in Fig. 6. Initially, energy depletion occurs in the border of each hop level. For the region in the second hop level, the residual energy of nodes in the area near to the first hop level becomes smaller rapidly.

The maximum energy consumption and the percentage of nodes connected to the sink in the first hop level are shown in Fig. 7. We observe the sharp increase of maximum energy consumption in the first hop nodes at  $t = 40$ , which is followed by the sudden loss of all network connections. Thus, by observing a rapid increase of the maximum energy consumption rate, we can predict

an immediate transition to complete network connection loss. Due to a large variation of workload in a dense deployment under a random parent selection scheme, we see that there is a substantial amount of time between the initial energy depletion of a node and the complete network disconnection.

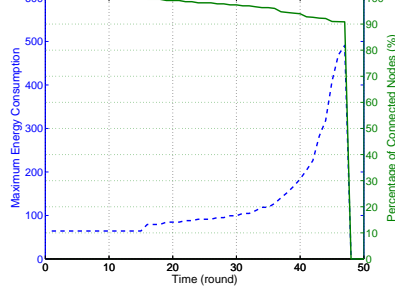


Fig. 7. The maximum energy consumption (the dashed line) and the percentage of nodes connected to the sink (the solid line) in the first hop level.

#### 4.3 Computer Simulation with Realistic Wireless Links

In this subsection, we perform computer simulation with 500 nodes and 100 different random deployments by incorporating a realistic wireless link model given in [23]. This model provides the packet reception rate along the distance by considering the path loss exponent, the shadowing effect, and the physical communication schemes. The key parameters used in the simulation are listed in Table 2.

Table 2

Parameters of realistic wireless link model (PRR: packet reception rate).

Parameters	Simulation Values
Transmitting power	-3dBm
Shadowing effect standard deviation	2
Path loss exponent	2.7
Transitional region start(PRR=0.9)	16.4m
Transitional region end(PRR=0.1)	38.5m
Modulation	FSK
Encoding scheme	MANCHESTER

The residual energy values of nodes at the same distance unit are averaged and plotted in Fig. 8 for each random deployment when 10% of nodes are disconnected from the sink. The figure presents the results of 100 runs. We see a large variation of residual energy values at the same distance. Even though a similar trend is observed by analysis described in Section 4.1 , the

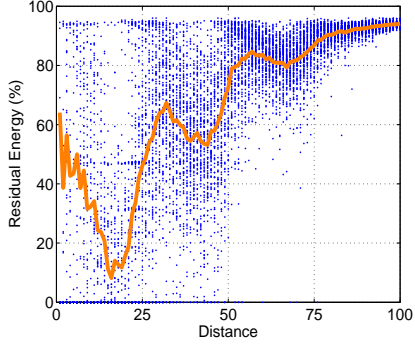


Fig. 8. The residual energy distribution at time with 10% connection loss. The solid line represents the average residual energy

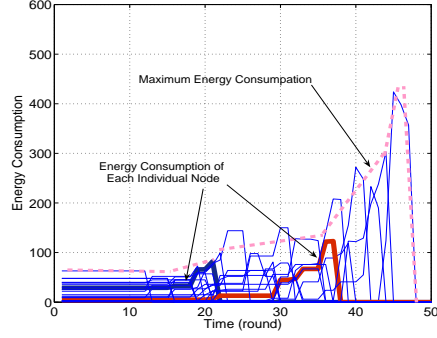


Fig. 9. Energy consumption of the first-hop nodes as a function of time. Each line represents the energy consumption of a node along time.

variation obtained by analysis is smaller. This can be explained by the fact that, besides the mixture of hop levels around the border areas, there exists a large variation in the number of children connected to nodes at the same distance in the simulation. The large variation of workload results in earlier death of some nodes in the second hop area as compared to that in analysis.

Simulation results of energy consumption of nodes in the first hop level as a function of time are shown in Fig. 9. Each line represents the energy consumption of a node in the first hop level along time. We see a wide range of variations in the initial energy consumption and the energy depletion time. Energy depletion of nodes with larger workload causes workload shift to remaining nodes. In addition, there exists a sharp increase of maximum energy consumption over time, which is consistent with the analytical result shown in Fig. 7.

The average residual energy over 100 simulation runs with random deployment is shown in Fig. 10, where each line represents a case when 1%, 5%, and 90% of the nodes are disconnected from a sink. Furthermore, analytical (indicated by dash lines) and simulation (indicated by solid lines) results are compared. Generally speaking, simulation and numerical results show similar pattern except for nodes in the border areas between two consecutive hop levels. In the simulation using a realistic wireless link model, some nodes in these border areas can be directly linked to a node in the upper hop level while others at the same distance cannot. As a result, the border area that is close to the next longer hop level in simulation has a higher residual energy than that obtained analytically. In contrast, the border area that is close to the upper hop level has a lower average residual energy in simulation than that in analysis. To conclude, the mixture of hop levels at the same distance around border areas due to a realistic wireless link model results in a smoother residual energy distribution along the distance from the sink.

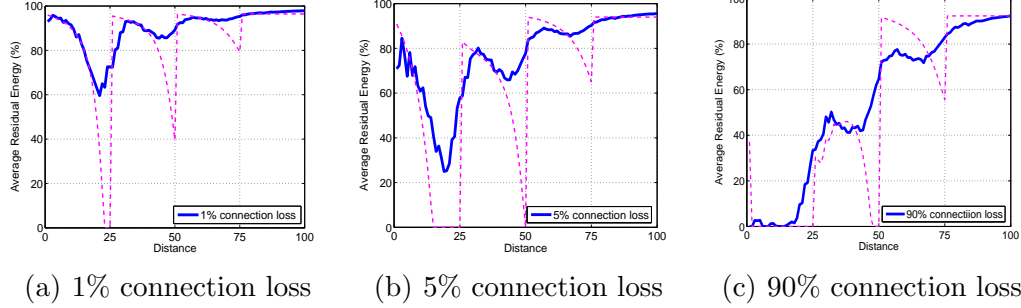


Fig. 10. The average residual energy with realistic wireless links, where analytical and simulation results are indicated by dash and solid lines, respectively.

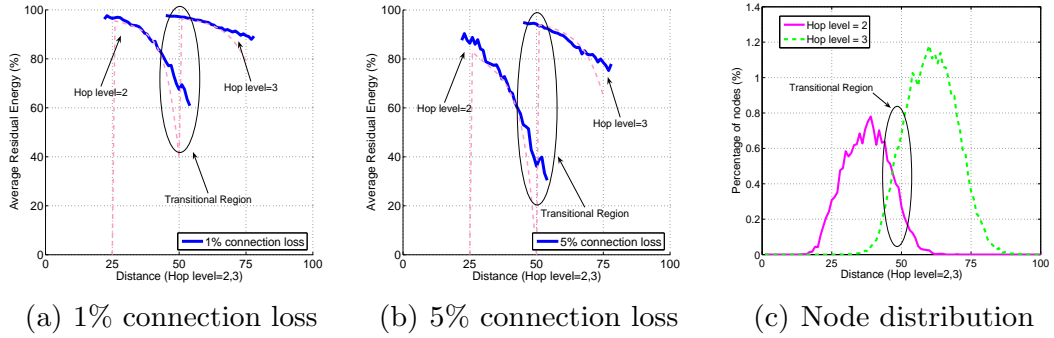


Fig. 11. (a),(b) The separate average residual energy of nodes in 2nd and 3rd hop levels with realistic wireless links. Analytical and simulation results are indicated by dash and solid lines, respectively, and (c) the distribution of 2nd and 3rd hop level nodes at each distance unit.

When the residual energy distributions of nodes in hop levels 2 and 3 are separated as shown in Fig. 11, we observe a good match between simulation and analysis results. Fig. 11(c) gives the node distribution in hop levels 2 and 3, which shows the mixture of hop levels in the border area from the distance 35 to 60, and around 90% of nodes in each hop level reside in the theoretical hop level.

To conclude, we observe a larger workload variation at the same distance level and a mixture of hop levels in the simulation using a realistic wireless link model. These factors lead to smoother energy consumption and residual energy distribution as compared to our analytical results. Generally speaking, results in simulation and analysis are consistent with each other in the general trend.

#### 4.4 First-hop Node Aging Analysis

As discussed in the previous sections, there exist workload differences among nodes in the same hop level using a random parent selection scheme for the

data gathering tree construction. This results in gradual energy depletion among nodes and workload shift from energy-depleted nodes to survivor nodes until the complete network connection loss is reached as shown in Fig. 9. Here, workload represents the amount of data packets to be handled by the node from its descendants in the data gathering tree in order to forward them to the sink. In this section, we characterize these aging phenomena, including energy depletion time and workload shift, of the first-hop nodes with closed-form expressions. In particular, we would like to address the following questions.

- (1) How does the workload of each survivor node in the first-hop change over time when some nodes with a higher workload deplete their equipped energy?
- (2) How to estimate the energy depletion time of nodes with a given workload distribution?
- (3) How much longer does a node with the smallest workload portion survive after the initial node death?
- (4) What is the effect of the node density and the radio range on the aging phenomenon?

Through a dynamic data gathering tree construction process, the workload of energy-depleted nodes in the first-hop level is re-distributed to remaining survivor nodes. Based on the observation in Section 4.1, the newly added workload is roughly proportional to the initial workload distribution. That is, since energy depletion occurs from the furthest distance from the sink in the first-hop, the amount of newly added workload to survivor nodes rises sharply as the distance from the sink increases since the region has more candidate children as given in Eq. (7). Thus, to simplify this first-hop analysis, we assume that the workload of each survivor node keeps increasing in proportion to the initial workload distribution by sharing the workload of energy depleted nodes.

The system model for the first-hop analysis and several basic properties can be stated below.

- When all nodes survive, the first-hop nodes are ordered by their workload  $1, 2, \dots, i, \dots, f$ , where  $f$  is the total number of first-hop nodes, and their workload probability distribution is given by  $p_1 \geq p_2 \geq \dots \geq p_f$  with  $\sum_{i=1}^f p_i = 1$ . As discussed in the previous section, workload of a node is approximately proportional to the number of descendants attached to the node in the data gathering tree. Workload probability indicates the ratio of its own workload to total workload that should be handled by all the first-hop nodes. We do not assume any specific workload distribution. It can be uniform for all first-hop nodes or different among nodes as discussed in the distance-level aging analysis in Section 4.1.
- Let  $N$  be the total number of nodes deployed and  $W$  be the total workload in the first hop per data gathering round. It is assumed that the total workload

in the first hop nodes is proportional to the data units generated by their descendants on a data gathering tree, which is identical to the number of descendants. Thus, we have  $W = \alpha(N - f)$ , where  $\alpha$  is a proportional constant.

- The workload of node  $i$  at data sampling round  $t$  can be computed as  $L_i(0) = Wp_i$ ,  $\sum_{i=1}^f L_i(t) = W$ .
- The energy depletion time of node  $i$  can have the following order:  $D_1 \leq D_2 \leq \dots \leq D_f$ , since the workload of a node determines its energy depletion time; Node with larger workload consumes energy faster. If all the first-hop nodes have the same portion of workload, then the energy depletion time would be the same.

By assuming that the workload of each survivor node keeps increasing in proportion to the initial workload distribution by sharing the workload of energy depleted nodes, we can obtain the workload function of node  $i$  over  $t$  as

$$L_i(t) = \begin{cases} Wp_i, & \text{if } 0 \leq t < D_1, \\ \frac{Wp_i}{1 - \sum_{m=1}^{j-1} p_m}, & \text{if } D_j \leq t < D_{j+1}, 1 \leq j < i, \\ 0, & \text{if } t \geq D_i, \end{cases} \quad (9)$$

where  $j$  indicates a node that has more workload than  $i$ .

Energy depletion time of node 1, which has the largest workload, can be obtained by  $D_1 = \frac{B}{Wp_1}$ , where  $B$  is the total workload of a battery. Furthermore, for node  $i \geq 2$ , its energy depletion time  $D_i$  can be obtained from  $D_{i-1}$  and the remaining battery capacity divided by its total workload that has been increased after  $D_{i-1}$  as

$$D_i = D_{i-1} + \frac{B - \sum_{m=1}^{i-1} ((D_m - D_{m-1})L_i(D_{m-1}))}{L_i(D_{i-1})}, \quad i \geq 2. \quad (10)$$

Actually, we can obtain the energy depletion time of node  $i$  using only the initial workload distribution without relying on the recursive formula shown in Eq. (10). That is,  $D_i$  can be written as

$$D_i = \frac{B}{Wp_i} \left( 1 + (i-1)p_i - \sum_{m=1}^{i-1} p_m \right), \quad i \geq 2, \quad (11)$$

which can be proved by induction as in Appendix C.

The energy depletion time of node  $f$ , which is the last surviving node with the smallest workload in the first hop level, can be computed by (11). That is, we have

$$D_f = \frac{Bf}{W} = \frac{B}{\alpha(N/f - 1)}, \quad (12)$$

which is the total battery energy divided by the average workload. According to this expression, the workload distribution does not affect the energy depletion time of the last survivor node, which is the time when a whole network is disconnected from the sink. This result leads to an interesting point. That is, by increasing or decreasing the node density with a fixed radio range to maintain the maximum hop levels, the disconnection time of the last first-hop node will remain the same. If we only consider the average workload in a hop level and the average energy depletion time of nodes in the same hop, the average energy depletion time of the first-hop nodes remains the same regardless of the node density. Our result does not deal with this trivial case of average time, but the complete network disconnection time that is the energy depletion time of the last survivor node. The calculation presented in Eq. (12) incorporates the dynamic changes of workload and its increasing rate, which are dependent on the earlier energy depletion times of all nodes with more workload, recursively as in Eq. (10). In addition, the above result holds for any arbitrary workload distribution.

Also, we can obtain the time duration of the aging process by measuring the ratio of the lifetime of node  $f$ , the last survivor node, and the lifetime of node 1, the first energy depleted node. From Eq. (10) and Eq. (12), we have  $\frac{D_f}{D_1} = f \cdot p_1$ , which depends on the number of first-hop nodes and the fraction of the largest workload. If perfect workload balancing can be performed on first-hop nodes, where  $p_i = 1/f$ , then the energy depletion time will be the same, which is desirable. Simultaneous energy depletion of first-hop nodes can also be achieved by heterogeneous energy capacity deployments according to workload.

## 5 Conclusion and Future Work

The aging process in a multi-hop data gathering tree with a sink was studied thoroughly in this work. Both hop-level analysis for sparse node deployment and finer-grained distance-level analysis for dense node deployment were examined. The effect of the workload distribution and the node density on the aging process in the first-hop nodes was also analyzed. Besides theoretical analysis, we provided simulation results using a realistic wireless link model.

Several important results are summarized below.

- For the hop-level analysis in a sparse node deployment, three conditions of node death; namely, energy depletion without data aggregation, with data aggregation and due to device failure, were examined for the connectivity aging per hop level over time. The existence of multiple alternate paths to the sink leads to a power law relation, where the probability of connection to the sink decreases in proportion to the hop level with an exponent, as node death occurs. This relation holds in the device failure case as well as in the late stage of the energy depletion case with data aggregation.
- By incorporating dynamic data gathering tree re-construction, aging analysis in densely deployed networks enables fast and accurate prediction of the energy consumption distribution and the residual energy distribution in a large-scale network over time after initial node death. Besides theoretical analysis, we provided simulation results using a realistic wireless link model presented by [23]. A good match between analytical and simulation results was demonstrated. Energy consumption in live nodes significantly changes over time as the data gathering tree as well as the hop level structure change due to node death.
- A network with a high node density can provide a resilient connection against node failure and energy depletion. However, there may exist high skew in the workload distribution among nodes in the same hop level. It was shown by the first-hop analysis that the increased node density with a fixed radio range does not affect the complete network disconnection time due to energy depletion of all first hop nodes.

There are several open problems to be studied in the future. First, we have not incorporated the MAC operations and transmission delay in analysis in our current research. If the duration of a sampling round is large, the effect of MAC contention would be relatively small. Second, no transmission range is adjusted in our analysis. If transmission range adjustment is allowed after a parent is randomly selected among the upper hop level, then faster energy depletion would occur in the outer region of each hop level. Finally, if different localized topology construction schemes are adopted as described in [20], it affects the aging process. However, the complete network disconnection due to energy depletion of all first-hop nodes will occur at a similar time as predicted by Eq. (12). The main difference would be the time of the initial energy depletion of a node with the largest workload.

In order to provide a long-term operation of wireless sensor networks that experience the aging phenomenon as studied in this work, aging control and network maintenance are needed so as to achieve the required information utility throughout the target period. Maintenance may involve a significant cost, which could be more than the initial deployment cost. As analyzed and characterized in our work, in the sparse node deployment case, frequent rede-

ployment will be needed to preserve the initial network performance since the small fraction of node death can cause the significant connectivity loss in the longer hop levels. On the other hand, dense node deployment can maintain the initial network connectivity from longer hop level until the most first-hop nodes die. Ultimately, we intend to provide a cost-effective maintenance plan that maximizes information extraction throughout a target long-term deployment period with overall cost and performance requirements.

## A Simulation Results for the Sparse Node Deployment Case

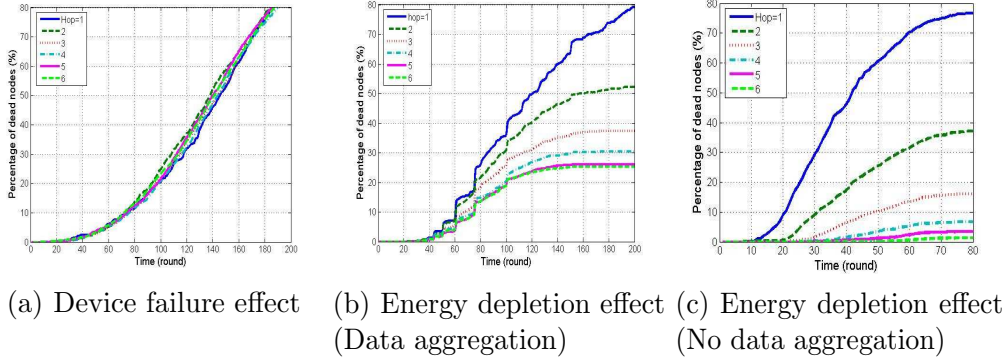


Fig. A.1. The percentages of dead nodes in each hop level over time: (a) the uniform random device failure case, (b) the energy depletion case with perfect data aggregation, and (c) the energy depletion case without data aggregation. Note that the  $x$ -axis scale in Fig. (c) is finer than that in Fig. (a) and (b).

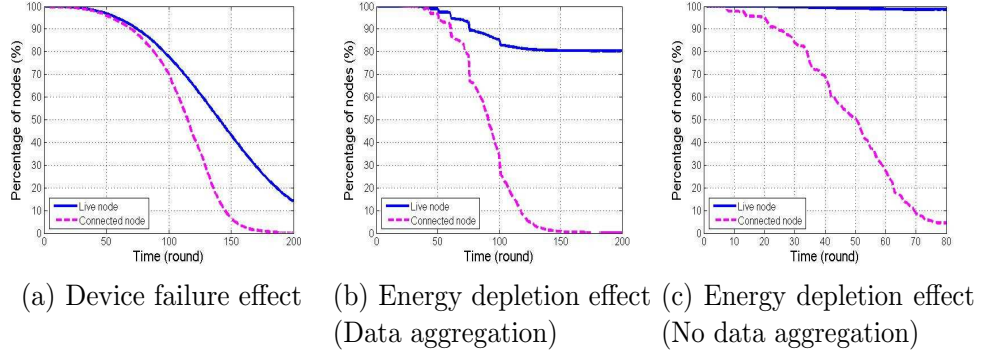


Fig. A.2. The percentages of live nodes and connected nodes in each hop level over time: (a) the uniform random device failure case, (b) the energy depletion case with perfect data aggregation, and (c) the energy depletion case without data aggregation. Note that the  $x$ -axis scale in Fig. (c) is finer than that in Fig. (a) and (b).

Fig. A.1 shows that a higher death rate appears in the hop levels closer to the sink in the energy depletion case. To simulate the energy depletion case without data aggregation, we increase the initial battery capacity 20 times as

large as that for the data aggregation case due to its faster energy depletion and network disconnection. We observe much faster energy depletion especially in the first-hop nodes as shown in Fig. 1(c) with the finer scale of the  $x$ -axis.

Fig. A.2 shows that, when the same ratio of nodes discontinue their functioning, the node death caused by energy consumption even with perfect data aggregation has a more significant impact on network performance than the device reliability effect. This figure presents the percentage of nodes connected to the sink in each hop level. A much lower degree of node death causes significant connection loss due to energy depletion. When no data aggregation is performed, the majority of connections are lost even with less than a 2% rate of node death. This is because significantly more workload is given to nodes in the first hop level as compared to the case of data aggregation.

## B Geometric Calculation for Dynamic Data Gathering Construction

The probability,  $Pr(A(c))$ , that a node at distance  $c$  from the sink selects one node in the upper hop area  $A(c)$  to the sink within its radio range was derived in [10] as  $Pr(A(c)) = \sum_{k=1}^{\infty} \frac{1}{k} Pr(N(A(c)) = k | N(A(c)) \geq 1) = \frac{e^{-\lambda A(c)}}{1 - e^{-\lambda A(c)}} \sum_{k=1}^{\infty} \frac{(\lambda A(c))^k}{k! k!}$ . Furthermore, areas  $C(d, c)$ ,  $D(c, t)$ ,  $A(c)$ ,  $A_1(c, t)$  and  $A_2(c, t)$  can be computed using geometry. These results are summarized as follows.

- Calculation of  $C(d, c)$ .

$$C(d, c) = \int_{c-\Delta d}^c 2 \cos^{-1}\left(\frac{d^2 + l^2 - r^2}{2ld}\right) l dl.$$

- Calculation of  $A(c)$ , which is the upper hop area within the radio range of a node at  $c$  distance from the sink.

First, we have  $w_{01} = \cos^{-1}\left(\frac{r^2 + c^2 - (hr)^2}{2rc}\right)$ ,  $w_{02} = \cos^{-1}\left(\frac{hr^2 + c^2 - r^2}{2hrc}\right)$ . Then, we obtain

$$A(c) = r^2(w_{01} - \sin(2w_{01})/2) + (hr)^2(w_{02} - \sin(2w_{02})/2).$$

- Calculation of  $A_1(c, t)$ , which is the area within  $A(c)$  except for the energy depletion area  $D(c, t)$  ( $= A(c) - A_1(c, t)$ ).

First, we have  $w_{11} = \cos^{-1}\left(\frac{r^2 + c^2 - d_{\max}^h(t)^2}{2rc}\right)$ ,  $w_{12} = \cos^{-1}\left(\frac{d_{\max}^h(t)^2 + c^2 - r^2}{2cd_{\max}^h(t)}\right)$ . Then, we get

$$A_1(c, t) = r^2(w_{11} - \sin(2w_{11})/2) + d_{\max}^h(t)^2(w_{12} - \sin(2w_{12})/2).$$

- Calculation of  $A_2(c, t)$ , which is the same hop area within the radio range of a node at  $c$ .

First, we have  $w_{21} = \cos^{-1} \left( \frac{(d_{\max}^{h-1}(t)+r)^2 + c^2 - r^2}{2c(d_{\max}^{h-1}(t)+r)} \right)$ ,  $w_{22} = \cos^{-1} \left( \frac{r^2 + c^2 - (d_{\max}^{h-1}(t)+r)^2}{2rc} \right)$ . Then, we find

$$A_2(c, t) = (d_{\max}^{h-1}(t) + r)^2 (w_{21} - \sin(2w_{21})/2) + r^2 (w_{22} - \sin(2w_{22})/2) - \{r^2 (w'_{01} - \sin(2w'_{01})/2) + ((h-1)r)^2 (w'_{02} - \sin(2w'_{02})/2)\}$$

where  $w'_{01}$  and  $w'_{02}$  are obtained by replacing  $h$  in  $w_{01}$  and  $w_{02}$  with  $h-1$ , respectively.

## C Proof of Energy Depletion Time of the First-hop Nodes

First, for  $i = 2$ , we have  $D_2 = D_1 + \frac{B - D_1 L_2(0)}{L_2(D_1)} = \frac{B}{Wp_1} + \frac{(B - (B/Wp_1)Wp_2)(1-p_1)}{Wp_2} = \frac{B}{Wp_2}(1 + p_2 - p_1)$ , where the second equality is due to Eq. (9). Thus, Eq. (11) holds for  $i = 2$ . Now, assuming that Eq. (11) holds for any integer  $k \geq 2$ , *i.e.*

$$D_k = \frac{B}{Wp_k} \left( 1 + (k-1)p_k - \sum_{m=1}^{k-1} p_m \right), \quad (\text{C.1})$$

we would like to prove that Eq. (11) also holds for  $D_{k+1}$ . The energy depletion time interval between  $k$  and  $k-1$  is

$$D_k - D_{k-1} = \frac{B}{W} \left( \frac{1}{p_k} - \frac{1}{p_{k-1}} \right) \left( 1 - \sum_{m=1}^{k-1} p_m \right). \quad (\text{C.2})$$

Furthermore, the consumed battery energy of  $k+1$  until  $D_k$  can be obtained using Eq. (C.2) and Eq. (9) as

$$\sum_{m=1}^k \left( (D_m - D_{m-1}) L_{k+1}(D_{m-1}) \right) = B p_k \sum_{m=2}^k \left( \frac{1}{p_m} - \frac{1}{p_{m-1}} \right) + \frac{B p_k}{p_1} = B \frac{p_{k+1}}{p_k}. \quad (\text{C.3})$$

The same result can also be obtained from the fact that  $L_{k+1}$  is increased while maintaining the ratio of  $p_{k+1}/p_k$  to  $L_k$  till node  $k$  reaches energy depletion. Thus, from Eq. (C.3), Eq. (9) and Eq. (C.1), we have

$$D_{k+1} = D_k + \frac{B - \sum_{m=1}^k \left( (D_m - D_{m-1}) L_{k+1}(D_{m-1}) \right)}{L_{k+1}(D_k)}$$

$$\begin{aligned}
&= \frac{B}{Wp_k} \left( 1 + (k-1)p_k - \sum_{m=1}^{k-1} p_m \right) + \frac{\left( B - B^{\frac{p_{k+1}}{p_k}} \right) \left( 1 - \sum_{m=1}^k p_m \right)}{Wp_{k+1}} \\
&= \frac{B}{Wp_{k+1}} \left( 1 + kp_{k+1} - \sum_{m=1}^k p_m \right)
\end{aligned}$$

Thus, we conclude that Eq. (11) holds for  $D_{k+1}$ . The proof is completed.

## Acknowledgment

This work was supported in part by NSF grants 0347621, 0325875, 0435505 and 0430061.

## References

- [1] C. Intanagonwiwat, R. Govindan, D. Estrin, Directed diffusion: A scalable and robust communication paradigm for sensor networks, in: Proc. ACM MobiCom'00, 2000.
- [2] D. Estrin, L. Girod, G. Pottie, M. Srivastava, Instrumenting the world with wireless sensor networks, in: ICASSP, 2001.
- [3] M. Rausand, A. Høyland, Longevity, Senescence and the Genome, University of Chicago Press, Chicago, 1990.
- [4] L. A. Gavrilov, N. S. Gavrilova, The biology of life span: a quantitative approach, New York: Harwood Academic Publisher, 1991.
- [5] L. A. Gavrilov, N. S. Gavrilova, The reliability theory of aging and longevity, Journal of Theoretical Biology 213 (2001) 527–545.
- [6] M. Rausand, A. Hoyland, System Reliability Theory: Models, Statistical Methods, and Applications, 2nd Edition, Wiley-Interscience, New Jersey, 2004.
- [7] B. Gompertz, On the nature of the function expressive of the law of human mortality and on a new mode of determining life contingencies, Philosophical Transactions 115 (1825) 513–585.
- [8] W. Heinzelman, A. Chandrakasan, H. Balakrishnan, Energy-efficient routing protocols for wireless microsensor networks, in: Proc. HICSS'00, 2000.
- [9] M. Bhardwaj, A. Chandrakasan, Bounding the lifetime of sensor networks via optimal role assignments, in: Proc. IEEE Infocom'02, 2002.

- [10] M. Lotfinezhad, B. Liang, Effect of partially correlated data on clustering in wireless sensor networks, in: Proc. IEEE SECON, San Jose, USA, 2004.
- [11] C.-F. Chiasserini, M. Garetto, Modeling the performance of wireless sensor networks, in: Proc. IEEE Infocom, Hong Kong, 2004.
- [12] Y. Chen, Q. Zhao, On the lifetime of wireless sensor networks, IEEE Communication letters 9 (2005) 976–978.
- [13] H. Zhang, J. Hou, On deriving the upper bound of  $\alpha$ -lifftime for large sensor networks, in: Proc. ACM MobiHoc, 2004.
- [14] S. Olariu, I. Stojmenovic, Design guidelines for maximizing lifetime and avoiding energy holes in sensor networks with uniform distribution and uniform reporting, in: INFOCOM, 2006.
- [15] Y. Chen, C. Chuah, Q. Zhao, Sensor placement for maximizing lifetime per unit cost in wireless sensor networks, in: MILCOM, 2005.
- [16] P. Gupta, P. R. Kumar, Critical power for asymptotic connectivity in wireless network, in: Stochastic Analysis, Control, Optimization and Applications, Birkhauser, Boston, 1998, pp. 547–566.
- [17] C. Bettstetter, On the minimum node degree and connectivity of a wireless multihop network, in: Proc. ACM MobiHoc'02, 2002.
- [18] S. Shakkottai, R. Srikant, N. Shroff, Unreliable sensor grids: Coverage, connectivity and diameter, in: Proc. IEEE Infocom'03, San Francisco, USA, 2003.
- [19] S. S. Kunniyur, S. S. Venkatesh, Network devolution and the growth of sensory lacunae in sensor networks, in: Modeling and Optimization in Mobile, Ad Hoc and Wireless Networks (WiOPT04), Cambridge, 2004.
- [20] C. Zhou, B. Krishnamachari, Localized topology generation mechanisms for self-configuring sensor networks, in: Proc. IEEE Globecom'03, San Francisco, USA, 2003.
- [21] V. Raghunathan, C. Schurgers, S. Park, M. B. Srivastava, Energy-aware wireless microsensor networks, IEEE Signal Processing Magazine 19 (2002) 40–50.
- [22] S. Madden, M. Franklin, J. Hellerstein, W. Hong, Tag: a tiny aggregation service for ad-hoc sensor networks, in: OSDI, 2002, pp. 131–146.
- [23] M. Zuniga, B. Krishnamachari, Analyzing the transitional region in low power wireless links, in: IEEE SECON, Santa Clara, 2004.